CAPTURE CAVITIES FOR THE CW POLARIZED POSITRON SOURCE Ce⁺BAF

*Shaoheng*Wang*, *Andriy* Ushakov, *Joseph* Grames, *Nabin* Raut, *Robert* Rimmer, *Yves* Roblin, and *Haipeng* Wang

[1]Thomas Jefferson National Accelerator Facility, Newport News, VA 23606, USA

Abstract. The initial design of the capture cavities for the continuous wave (CW) polarized positron beams at Jefferson Lab (Ce⁺BAF) is presented. A chain of standing wave multi-cell copper cavities inside a solenoid tunnel are selected to improve the positron capture efficiency. The cavity design strategy is presented to accommodate constrains from the large phase distribution of the incident beams, RF power and RF heating. A matrix of design parameters' range are given for future system optimization when the capture cavities are considered together with other sub-systems and beam dynamics. The contents will also be useful for other CW cavity design for beams with large phase space distribution.

1 Introduction

The CEBAF accelerator provides high energy spin-polarized electron beams, in addition, Jlab is now exploring an upgrade which would provide high energy spin polarized positron beams to address new physics [1, 2]. The PEPPo (Polarized Electrons for Polarized Positrons) technique is adopted [3] to generate the positrons. Here the spin polarization of an electron beam is transferred by polarized bremsstrahlung and polarized e+/e- pair creation within a high-power rotating tungsten target. A high current >1 mA spin polarized CW electron beam is produced, accelerated to an energy of 123 MeV and transported to the high-power target to generate the spin polarized positrons. A capture section, including a solenoid tunnel, shield and capture cavities will collect positrons to maximize intensity or polarization. Afterward the positrons will be separated from electrons by a chi-cane and further accelerated in the super conducting cavities to 123 MeV. The positrons are then accelerated by CEBAF accelerators up to 12 GeV and to any of the four halls. The Ce⁺BAF design is optimized to provide users with spin polarization >60% at intensities >100 nA, and with higher intensities when polarization is not needed.

2 CW CAPTURE LINAC

From the target, the positron source has small transverse dimensions, but large angular divergence and broad energy spread resulting from the shower processes and from multiple

*wang@jlab.org. This material is based upon work supported by the U.S. Department of Energy, Office of Science, Office of Nuclear Physics under contract DE-AC05-06OR23177

scattering. A Quarter Wave Transformer (QWT) is chosen as the matching device after the source which has a narrow band final energies. The beam size is increased and the beam occupies the geometrical acceptance at the entrance of the capture cavity. The RF capture section is used to increase the capture efficiency by decreasing the longitudinal energy spread and the transverse beam emittance. The whole capture linac is encapsulated inside a solenoid chain, which focuses the positrons and avoid losses while the RF accelerating field providing the longitudinal compression.

Because the capture Linac will be located inside the solenoid magnetic field, a copper cavity will be used. One special point of $Ce^{+}BAF$ is that it provides CW positron beams. Obviously, the copper cavity will also need to work in CW mode so the copper cavity wall loss power becomes a big challenge, which limits the maximum RF field gradient. In Travelling Wave capture cavity, the decelerating mode in the first capture cavity was proposed in 1979 by Aune and Miller [4] and applied later to improve the capture rate. This is not efficient in CW operation mode where gradient is very critical, so Standing Wave (SW) cavities will be used in this case.

In general, high-gradient and large-aperture cavities are required to ensure sufficient longitudinal and transverse acceptance for the positron beams. But with given RF wall loss power, the achievable RF field gradient is lower with larger iris aperture, the shunt impedance is lower. A large iris aperture also allows the high order modes to propagate out. The choice of the iris aperture and the available gradient need to be weighed and balanced with beam dynamics analysis. Variation of geometry of the RF cavities along the capture path is expected to maximize the capture rate.

In the starting part of the capture process, the electron bunches are coincident with the positron bunches. The beam loading effect is therefore alleviated by the beam current cancellation. Later on the electrons will be bunched at their own acceleration phase, half-RF wave-length away from the positron bunches, as indicated in Vallis' simulation [5]. With the addition of beam loss in the capture process, the ending part of the capture Linac will see different beam loading from the beginning. Different Forward Power Coupler (FPC) coupling factors will be needed for the RF cavities.

3 CAPTURE CAVITY DESIGN

3.1 Strategy

This is an RF cavity design as part of a larger system optimization. Therefore at this time the goal is not to produce a single design but to provide a range of options with given inputs from other parts of the project, within practical engineering constraints. With high-performance computing power available nowadays, a matrix of cavity designs can be produced, which can be used as input to further studies combined with beam dynamics tracking, RF and radiation thermal calculation, focusing solenoids and cooling design to pursue the best performance of the whole system. At the same time, this kind of survey work is also beneficial for similar CW normal conducting cavity designs for other projects.

Because it will be a multi-cell cavity, we also must make sure mode separation near π mode is large enough for possible high beam loading operation. Multi-cell cavities with two types of cell shapes are investigated, type A with simpler structure, larger cell-to-cell coupling, and type B with nose cone and typically higher shunt impedance are illustrated in Fig. 1. The correlation between the various geometry parameters, the shunt impedance and mode separation are surveyed. This set of cavity design works as a database for capture process beam dynamics analysis, particle shower radiation thermal analysis in next work phase.

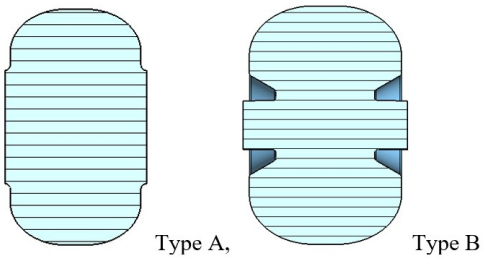

Figure 1: Cell shapes

3.2 Multi-Cell Cavity

The frequency of the RF cavity is 1497 MHz, the same as CEBAF. The cell number of the multi-cell cavity may be up to 11 to balance between the required RF power for each cavity, flexibility of the Linac configuration, over all effective gradient and mode separation near π mode. The gradient and phase from cavity to cavity could be used to tune the capture rate in later beam capture process analysis. But the cell number is not fixed and could be changed later as a result of such optimization.

Two waveguides are symmetrically connected to the middle cell of the cavity. Currently only a basic FPC design is performed, a tapered waveguide and cavity-to-waveguide iris connect the waveguide to the cavity, as shown in Fig. 2. It will be updated later when more detailed beam loading information becomes available. Initial results show that the maximum power density near waveguide iris won't be the limiting factor of the gradient.

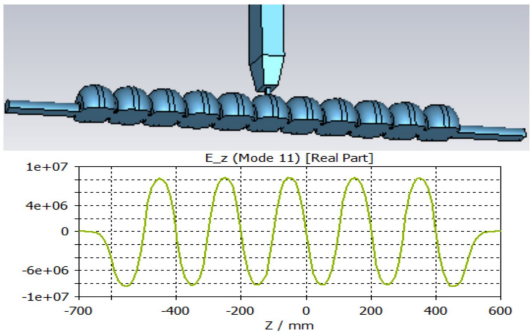

Figure 2: Example of an 11-cell capture cavity

The cell geometry survey starts with a structure of inner cells, as shown in Fig. 3. It has three resonators and is much simpler compared to the full cavity. The three calculated eigen modes of this structure will produce the cell-to-cell coupling information, and the mode separation near π mode for the multi-cell cavity can be derived. In the survey, when the geometry parameters are varied during the parameter scanning, the π mode resonance frequency deviates from 1497 MHz, it needs to be moved back by tuning the equator radius. A CST macro is written to combine the parameter scanning and the optimization at each parameter setting, which greatly improves the computational efficiency.

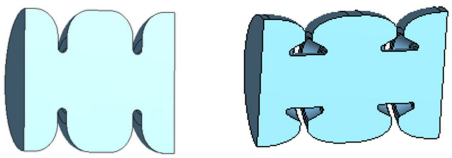

Figure 3: Inner cell structure for geometry survey

For both types of cavities, the center coupling cell and the two end cells are not identical to the inner cells, their equator radii are tuned so the field levelness can be achieved. Then the full cavity model is obtained.

3.3 Inner-Cell Geometry Survey

For type A cell cavity, the iris radius, equator ellipse axes and cell wall thickness are varied. For type B cell cavity, the iris radius, nose gap length, nose cone angle, nose cone tip straight height and equator ellipse axes are varied. The shunt impedance and mode separation near π mode are recorded for each variant. The results are shown in Fig. 4, 5, 6, 7, 8. For the shunt impedance, we can see that, the iris radius has the most significant impact for both types of cavities. The shunt impedance of type B cavity is higher than that of type A cavity, but not significantly for cases with iris radius larger than 30 mm. Nose cone tip and gap in type B cavity also change the impedance noticeably. The equator radius also influences the impedance for both type of cavities. The cell wall thickness doesn't contribute much. For 1 MV/m effective gradient, RF power about 50 kW per cavity is needed. Type A cavity has much higher mode separation near π mode than type B cavity. Decreasing the cell number in type B cavity can help widen the mode separation near π mode. The net result is a continuous trade-off between iris radius (transverse acceptance of the positrons) and gradient (energy acceptance). At small radii the nose-cone cavity is more efficient, at larger radius the simple iris cavity is sufficient. This parameterization can now be used in the capture dynamics simulations to maximize total acceptance into Ce^{+}BAF.

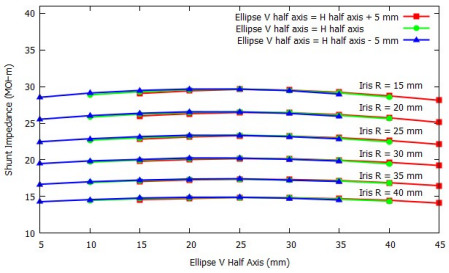

Figure 4: Shunt impedance, type A cell

4 Initial Beam Dynamics Results

GEANT4 [6] is used for the positron production simulation in the target, and the positrons exit the back face of the target is used as the initial distribution for positron beam dynamics

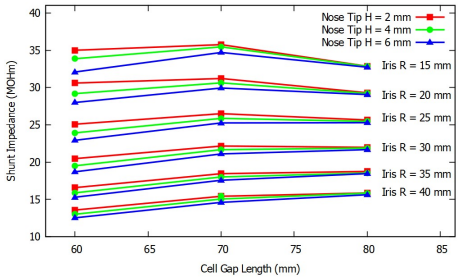

Figure 5: Shunt impedance, type B cell

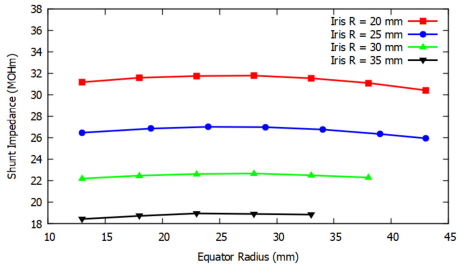

Figure 6: Shunt impedance vs equator radius, type B cell

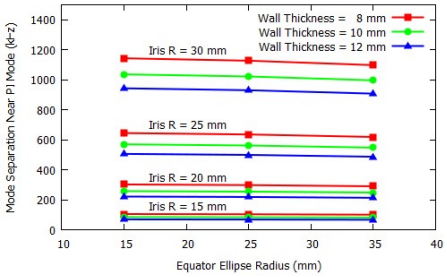

Figure 7: Mode separation near π mode, type A cavity

study in the matching and capturing section, as shown in Fig. 9. The magnetic field is produced with a bucking solenoid, a focusing solenoid S1 with 1.02 T peak flux intensity and a long weak cavity solenoid S2 covering the cavity length. With the bucking solenoid, zero magnetic flux intensity is realized at the target location. This setup ensures the production of non-magnetized positron beam is produced. Without the bucking solenoid, the canonical angular momentum introduced by the high intensity focusing solenoid S1 would manifest as the mechanical angular momentum in the long transportation section after the capture cavity solenoids and increase the effective transverse emittances.

One RF cavity with 3 MV/m peak on-axis gradient is used in the study. There are two reasons to study the beam dynamics with one capture cavity. The first is the simplicity. The second is to use the extendability of the capture cavity optics. Both solenoid and capture cavities can not be continuous over long distance. If the positron bunches can be imaged

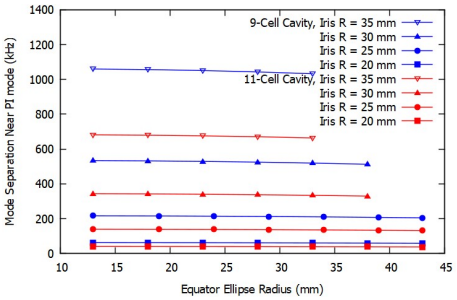

Figure 8: Mode separation near π mode, type B cavity

in every gap between the cavities, then they can be transported over longer distance without significant loss. The optics transportation matrix for each section of the cavity and solenoid must be fine tuned for positron beam of certain energy.

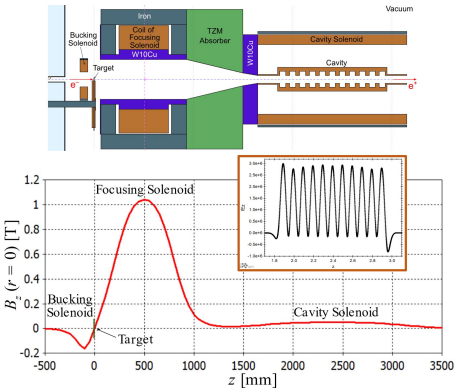

Figure 9: Geometry of target and beginning of positron capture system

In this first matching-capturing section, the length and magnetic flux intensity of the focusing solenoid S1 is tuned to maximize the passing through rate for a certain energy, here it is 60 MeV. For positrons of energy far away from 60 MeV, or with large initial emitting angle, they will get lost soon or later, as shown in the top row of Fig. 10. The magnetic mirror effect is also observed in the simulation, as shown in the bottom left graph of Fig. 10. Positrons whose velocity vectors lie outside the loss cone are reflected back to the target. The information of these lost particles are important for the thermal and radiation consideration.

In this paper, authors are more concerned about the capturing capability of the normal conducting RF cavities operating in CW mode, so the matching and fine tuning of the solenoid field will postponed to next step of work. Two energy bands, near 20 MeV and 60 MeV, of positrons traveled to the entrance of the cavity are selected for further transportation through the capture cavity. Their energy gain, particle number, transverse and longitudinal brightness are obtained at the exit of the cavity and compared with no RF field case. The results are shown in Fig. 11 and Fig. 12. The RF phase of the cavity varies to find the extreme results. We can see that the pass through rate is significantly improved for 20 MeV case, but not the 60 MeV case. So, for 20 MeV case, it is worth to further study the improvement from fine

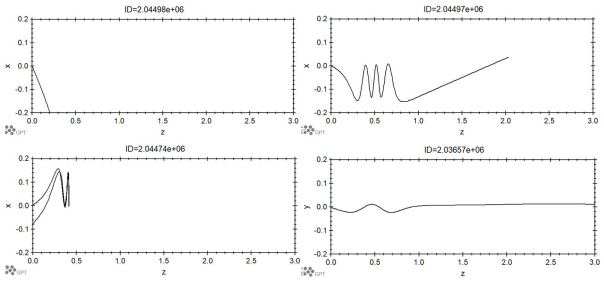

Figure 10: Top: positrons lost; bottom left: position reflected back to target; bottom right: positrons going through the cavity

tuning solenoids and with more cavities. For 60 MeV case, we need to use a short version QWT to pass the positrons earlier into SRF cavity, more studies is needed for the details.

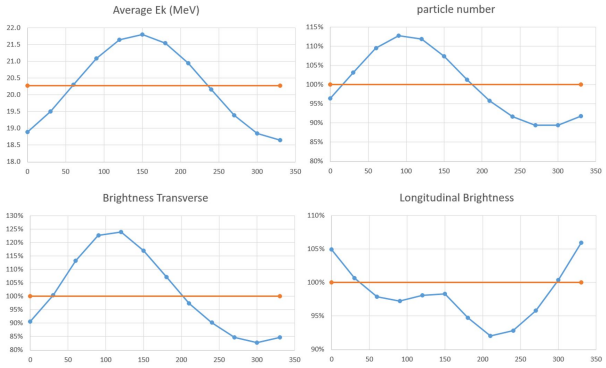

Figure 11: Positrons with energy near 20 MeV. The horizontal axis is the RF phase of the cavity.

5 CONCLUSION

A parameter survey for two types of standing wave capture cavities has been performed for CW positron source. Different cavity geometry can be chosen for further beam dynamics, higher order modes analysis and thermal analysis in the next phase of work. The survey results are also valuable for other applications with CW copper cavities. Initial beam dynamics studies show that normal conducting RF cavities are applicable for capturing positron of energy near 20 MeV in $Ce^{+}BAF$ case. A short version QWT is needed to pass the 60 MeV positrons earlier into SRF cavity, more studies is needed for the details.

References

[1] J. Grames et al., "Positron beams at $Ce^{+}BAF$", in Proc. 14th Int. Particle Accelerator Conf. (IPAC'23), Venice, Italy, May 2023. pp. 896–899.

[2] A. Ushakov, et al, "Simulations of Positron Capture at $Ce^{+}BAF$", presented at the 14th International Particle Ac-celerator Conf. (IPAC'24), Nashville, Tennessee, USA, May 2024.

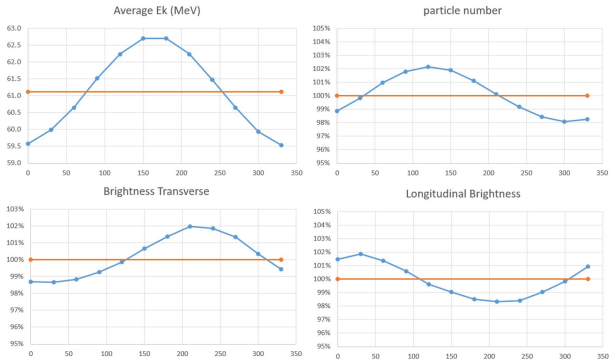

Figure 12: Positrons with energy near 60 MeV. The horizontal axis is the RF phase of the cavity.

[3] D. Abbott et al, “Production of Highly Polarized Positrons Using Polarized Electrons at MeV Energies,” Phys. Rev. Lett. **Volume** 116, 214 (2016).

[4] B. Aune, R.H. Miller, "New Method for Positron Production at SLAC", SLAC-PUB-2393, USA, 1979.

[5] N. Vallis , et al, “Proof-of-principle e + source for future colliders”, PHYSICAL REVIEW ACCELERATORS AND BEAMS **Volume** 27, 013401 (2024).

[6] https://geant4.web.cern.ch/